

Available online at www.sciencedirect.com

ScienceDirect

Procedia CIRP 71 (2018) 354–357

www.elsevier.com/locate/procedia

4th CIRP Conference on Surface Integrity (CSI 2018)

Residual stresses in grinding of forming tools with toric grinding pins

Thilo Grove^a, Henning Lucas^{a,*}, Berend Denkena^a^aInstitute for Production Engineering and Machine Tools, Leibniz Universität Hannover, An der Universität 2, D-30823 Garbsen, Germany* Corresponding author. Tel.: +49-511-762-18002; fax: +49-511-762-5115. E-mail address: lucas_h@ifw.uni-hannover.de

Abstract

The subsurface residual stress state of forming tools is an important factor for the lifetime of these tools. This is especially important for tools used in processes like sheet-bulk metal forming, where very high process loads occur in the tools during the forming operation. Grinding as one of the last process steps for manufacturing of these tools significantly affects the subsurface residual stress state. For five-axis grinding, toric tools are advantageous, because constant contact conditions are realized even on complex free form surfaces. Previous work identified the major process and tool parameters for influencing the residual stress state due to grinding with toric grinding pins.

This paper investigates the quantitative correlations between the main parameters feed rate and cutting grain size and the resulting residual stresses in a full factorial experimental design for the lateral grinding strategy. An empirical model is determined from the results of the experiments, which allows to predict these residual stresses for toric pin grinding. Additional grinding force measurements and cutting simulations are conducted to gain additional insight in the generation of residual stresses through grinding with toric pins.

© 2018 The Authors. Published by Elsevier Ltd. This is an open access article under the CC BY-NC-ND license

(<https://creativecommons.org/licenses/by-nc-nd/4.0/>)

Selection and peer-review under responsibility of the scientific committee of the 4th CIRP Conference on Surface Integrity (CSI 2018).

Keywords: grinding; residual stresses; toric tools

1. Introduction

The application of different manufacturing processes to influence the subsurface of a machined part with the aim of inducing additional functionality is a major goal of today's research in manufacturing technology [1]. One of the most important subsurface properties which leads to improved functionality of a part is the residual stress state of the subsurface. Compressive residual stresses inhibit crack initiation and propagation under cyclic load and can therefore enhance the lifetime of forming tools [2]. Due to its high contact pressures the new manufacturing process sheet-bulk metal forming is a good example for the need of optimized forming tool properties [3].

Forming tools for this process are made of high alloyed tool steels. Hard machining after hardening is usually done by either grinding or electrical discharge machining (EDM) and a final polishing step to achieve the needed high surface finish. While EDM is known to induce unfavorable tensile residual stresses into the subsurface [4], grinding is able to induce high compressive residual stresses [5]. Grinding with special toric

grinding pins is able to machine complex geometries with constant contact conditions and therefore able to generate a constant surface integrity [6]. Grinding with toric tools is therefore an excellent process for the manufacturing of forming tools for the sheet-bulk metal forming process as well as inducing the necessary compressive residual stresses to enhance tool life.

1.1. Grinding with toric grinding pins

In Fig. 1 the principal process parameters for grinding with toric tools can be seen. One of the distinctive features of grinding with toric pins is the grinding strategy. It can be divided into two extremes. When feed rate v_f and cutting speed v_c have the same direction, the strategy is called lateral. When feed rate v_f and cutting speed v_c are transverse to each other, the strategy is called frontal. In a previous work the significance of the influence of the following tool and process parameters was investigated: grinding grain size d_G , grain concentration C , bonding type B , grinding strategy S , cutting speed v_c and feed rate v_f . Grinding strategy, grain size and

feed rate were shown to be the only parameters with significant influence on the resulting residual stresses [5]. Grain size and feed rate for the lateral strategy are therefore further investigated in this paper. The aim of this work is the accurate prediction of the induced residual stresses with an empirical model.

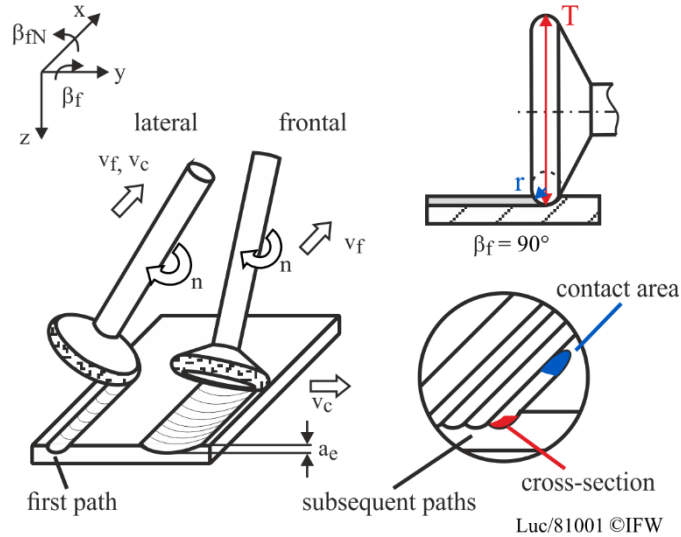


Fig. 1. Depiction of principle parameters for grinding with toric pins

Nomenclature

a_e	depth of cut
a_b	path distance
d_G	grinding grain size
r	torus minor radius
T	torus main diameter
v_c	cutting speed
v_f	feed rate
β_f	lead angle
β_{fN}	tilt angle
σ_{\parallel}	residual stresses parallel to cutting direction (v_c)
σ_{\perp}	residual stresses transverse to cutting direction (v_c)

2. Experimental setup

Samples from AISI M3:2 steel (1.3344 PM) with a hardness of 63 HRC were used for the experiments. The samples were hardened and quenched by vacuum hardening and had no preliminary residual stresses. For all grinding experiments ceramically bonded tools with a grain concentration of $C = 125$, a main diameter of $T = 30$ mm and a minor radius of $r = 5$ mm were used. All grinding experiments were conducted on a Rödgers RFM 600 DS machine tool. Cutting speed and depth of cut were kept constant at $v_c = 35$ m/s and $a_e = 50$ μm , respectively. The tilt angle for the lateral grinding strategy was chosen as $\beta_{fN} = 30^\circ$. For the lateral strategy, the minor radius of the tool is in the same plane as the path distance, resulting in smaller grinding grooves in comparison to the frontal grinding strategy (see Fig. 1). To achieve a small macroscopic roughness depending on the tool geometry a path distance of $a_b = 100$ μm was chosen.

2.1. Design of experiment

A full factorial design for grain size and feed rate was investigated. The grain size was varied in four steps $d_G = 15$ μm , 54 μm , 76 μm , 91 μm . Feed rate was investigated in four steps as well $v_f = 50$ mm/min, 250 mm/min, 500 mm/min, and 2000 mm/min. Additional experiments were performed at $v_f = 1000$ mm/min to validate the developed model. For each parameter combination five experiments were conducted to achieve higher statistical certainty.

2.2. Analytical methods

Process forces were measured using a dynamometer type Kistler 9256A2. The measurement was evaluated using an IFW internal software tool for LabVIEW from National Instruments. Force maxima and averages were calculated for normal and tangential directions of the grinding process.

Residual stress measurements were conducted via X-ray diffraction using the $\sin^2\psi$ -technique described by Macherach and Müller[7]. A General Electric Seifert XRD 3003 TT diffractometer with Cr-Anode and V-Filter at acceleration voltage of $U_a = 30$ kV and anode current of $I_a = 35$ mA was used. The measuring spot was 2 mm in diameter. Measurements were done parallel and transverse to the cutting direction. These correspond to the two principle residual stress directions for the grinding process as shown in [5].

3. Experimental results

Experiments with $d_G = 15$ μm and $v_f = 2000$ mm/min were excluded from analysis due to high tool wear and strong grinding burn on the workpiece surface. It was not possible to achieve a stable process.

3.1. Contact conditions

Removal rate, cross-section and contact area for the experiments were calculated for subsequent paths after the first and are listed in Table 1. The contact area between tool and workpiece cannot be calculated easily by analytical means due to the distortion of the contact ellipsoid when tilting the tool via the lead or tilt angle. Therefore, it was computed using the material removal simulation software

Table 1. grinding parameters

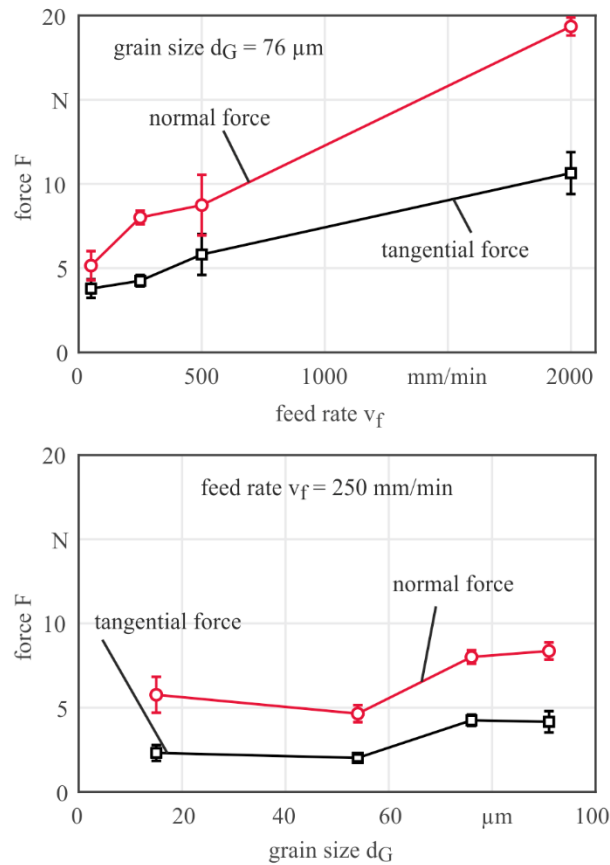
feed rate v_f (mm/min)	cross-section (mm ²)	contact area (mm ²)	material removal rate (mm ³ /s)
50	$4,93 \cdot 10^{-3}$	$378 \cdot 10^{-3}$	$4,1 \cdot 10^{-3}$
250	$4,93 \cdot 10^{-3}$	$378 \cdot 10^{-3}$	$20,5 \cdot 10^{-3}$
500	$4,93 \cdot 10^{-3}$	$378 \cdot 10^{-3}$	$41,1 \cdot 10^{-3}$
2000	$4,93 \cdot 10^{-3}$	$378 \cdot 10^{-3}$	$160,43 \cdot 10^{-3}$

“IFW – CutS”. The contact area is much bigger than the cross section of the tool and the workpiece (see Fig. 1). This is due

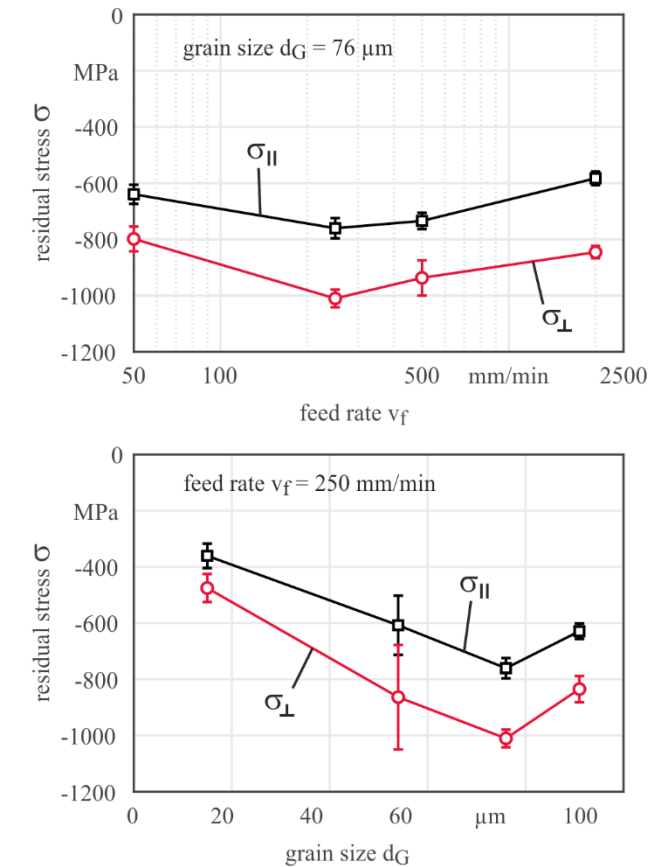
to the high torus diameter in comparison to the depth of cut of $a_e = 50 \mu\text{m}$.

3.2. Grinding forces

Tangential and normal grinding forces are depicted exemplarily for all feed rates for $d_G = 76 \mu\text{m}$ and all grain sizes for $v_f = 250 \text{ mm/min}$ in Fig. 2. As expected grinding forces continuously rise with an increase of material removal rate. The single grain has to cut more material and therefore generates higher forces. Grinding forces do not change significantly with grain size. With increasing grain diameter the volume of the single grain increases with a power of three, while the surface area only increases with quadratic power. Since the overall volume of cutting grains in each tool is the same, a higher grain diameter also results in a reduced number of grains. This would usually lead to smaller forces due to a smaller share of energy consumption by friction on the single grain. For the small forces measured in these experiments, however, this effect cannot be observed.



transvers to cutting direction are always higher than residual stresses parallel to cutting direction. While the grinding forces vary stronger with the feed rate, the residual stresses show a higher dependency on the grain size. Differences in residual stress values depending on the feed rate are only 200 MPa at maximum. Since the residual stress measurements for experiments with the same parameters have a relatively high variation, no clear trend was observed. There was an optimal feed rate around the mid range to achieve maximum compressive residual stresses for $d_G = 76 \mu\text{m}$. For all other grainsizes the maximum residual stresses were measured for $v_f = 50 \text{ mm/min}$. The higher grinding forces due to higher feed rates do not show any significant effect on the residual stresses. Most of these forces act on parts of the workpiece, which are removed later and are not part of the remaining subsurface. The slightly lower compressive residual stresses for $v_f = 250 \text{ mm/min}$ in all experiments are probably a result of higher temperatures in the grinding process. Further investigations are necessary to confirm this.



tilt angle: $b_{fN} = 30^\circ$ μm grain size: $d_G = \text{var.}$
 cutting speed: $v_c = 35 \text{ m/s}$ feed rate: $v_f = \text{var.}$
 depth of cut: $a_e = 50 \mu\text{m}$

Luc/91063 ©IFW

Fig. 3. Selected residual stresses depending on feed rate and grain size

tilt angle: $b_{fN} = 30^\circ$ μm grain size: $d_G = \text{var.}$
 cutting speed: $v_c = 35 \text{ m/s}$ feed rate: $v_f = \text{var.}$
 depth of cut: $a_e = 50 \mu\text{m}$

Luc/91062 ©IFW

Fig. 2. Selected grinding forces depending on feed rate and grain size

3.3. Residual stresses

The results of the residual stress measurement can be seen in Fig. 3. For all experiments, compressive residual stresses were detected in the surface near subsurface. Residual stresses

The differences in dependency of the grain size are much more prominent. For a feed rate of $v_f = 250 \text{ mm/min}$ the margin between the residual stresses transverse to cutting direction for $d_G = 15 \mu\text{m}$ in comparison to $d_G = 76 \mu\text{m}$ are more than 500 MPa. As described in section 3.2 bigger grains have to achieve the same material removal rate with fewer grinding grains cutting and less overall cutting face area. The

overall stress which the single grain induces into the material is therefore higher, resulting in higher plastic deformation of the subsurface area and concluding in higher compressive residual stresses. If the grain size exceeds an optimal value, no more additional residual stresses are induced into the material. Cutting forces for $d_G = 91 \mu\text{m}$ did not exceed the forces for $d_G = 76 \mu\text{m}$ either, so it can be assumed that the even higher stresses on the single grain rather lead to a higher heat generation, than more plastic deformation.

A calculation of the average chip thickness as proposed by Lierse [8] does not have any benefit here. Higher feed rates as well as a higher grain size both increase the average chip thickness. As mentioned earlier most of this additional grinding work is done in a part of the workpiece, which is removed later by a rear part of the tool. This additional work may have an impact on the temperature in the workpiece and must be further investigated by experiments measuring the workpiece temperature. In comparison, the last grinding grains in contact with the finished subsurface principally induce plastic deformation. It is therefore largely independent of the increase of average chip thickness, which occurs in the later removed part of the workpiece.

All experimental results were used to calculate a prediction model for the residual stresses using linear regression. Variables were logarithmically transformed to achieve a better fit. The following equation is used to predict the residual stresses:

$$\sigma_{ESP} = -\exp(b_1 d_G^2 + b_2 * d_G + b_3 * v_f + c) \quad (1)$$

Coefficients for both residual stresses parallel (σ_{\parallel}) and transverse (σ_{\perp}) to cutting direction are summarized in Table 2. Additional experiments for every grain size with a feed rate of $v_f = 1000 \text{ mm/min}$ were conducted and compared to the predictions of the model (see Fig. 4). The arithmetic mean of all measured residual stresses lies within a range of less than 50 MPa of the prediction and therefore inside the standard deviation (see Fig. 4). The single measurement might deviate further from the model, since experiments with same parameters are still dispersed over roughly 200 MPa from maximal to minimal value.

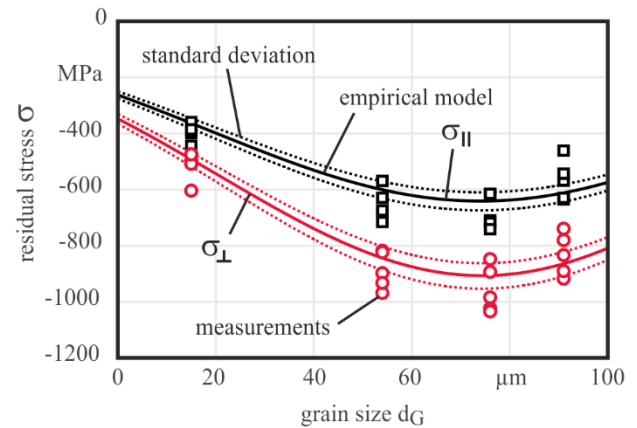
Table 2. Coefficients for empiric prediction model

	σ_{\parallel}	σ_{\perp}
b_1	$-1,62752 \cdot 10^{-4}$	$-1,73507 \cdot 10^{-4}$
b_2	$2,41 \cdot 10^{-2}$	$2,58 \cdot 10^{-2}$
b_3	$-8,77145 \cdot 10^{-5}$	$-3,69065 \cdot 10^{-5}$
c	5,6585	5,8876

4. Conclusion and outlook

Cutting grain size and feed rate, the major influences on the subsurface residual stress state when grinding with toric grinding pins, were examined for the lateral grinding strategy. Both, feed rate and grain size, show significant influence on the compressive residual stresses present after the grinding with grain size as the dominant factor. A model was derived via regression from the experiments, which successfully predicts the residual stresses within reasonable accuracy. The

high variance of the measured values for the residual stresses for the five experiments done with the same parameters point out, that a higher process stability would further refine the model. Furthermore, the frontal strategy needs to be examined as well and compared to the findings for the lateral strategy. Lastly, further experiments are needed to physically explain



tilt angle: $b_{fN} = 30^\circ$ grain size: $d_G = \text{var.}$
cutting speed: $v_c = 35 \text{ m/s}$ feed rate: $v_f = \text{var.}$
depth of cut: $a_e = 50 \mu\text{m}$

Luc/91064 ©IFW

Fig. 4. Intersection of the regression model at $v_f = 1000 \text{ mm/min}$

the model and to achieve wider validity.

Acknowledgements

The authors would like to thank the German Research Foundation (DFG) for the funding of the subproject B8 “Grinding strategies for local and stress orientated subsurface-modification of sheet-bulk metal forming tools” as part of the Transregional Collaborative Research Centre on sheet-bulk metal forming (SFB/TR 73).

References

- [1] Jawahir IS, Brinksmeier E, M'Saoubi R, Aspinwall DK, Outeiro JC, Meyer D, Umbrello D, Jayal AD. Surface integrity in material removal processes: Recent advances. CIRP Annals-Manuf Technol 2011;60:603-626.
- [2] Lange K, Kammerer M, Pöhland K, Schöck J. Fließpressen, 1st ed. Berlin: Springer, 2008
- [3] Merklein M, Koch J, Opel S, Schneider T. Fundamental investigations on the material flow at combined sheet and bulk metal forming processes. CIRP Annals-Manuf Technol 2011;60: 283-286.
- [4] Garcia Navasa V, Ferreres I, Marañón JA, Garcia-Rosales C, Gil Sevillano J. Electro-discharge machining (EDM) versus hard turning and grinding - Comparison of residual stresses and surface integrity generated in AISI O1 tool steel. J Mat Pro Tec 2008;195:186-194.
- [5] Denkena B, Grove T, Lucas H. Influences of grinding with Toric CBN grinding tools on surface and subsurface of 1.3344 PM steel. J Mat Pro Tec 2016;229:541-548.
- [6] Denkena B, Köhler J, van der Meer M. A roughness model for the machining of biomedical ceramics by toric grinding pins. CIRP J. Manuf. Sci. Technol 2013; 6: 22-33.
- [7] Macherach E, Müller P. Das $\sin^2\psi$ -Verfahren der röntgenographischen Spannungsmessung Zeitschrift für angewandte Physik 1961;13 (7) :305-312
- [8] Lierse T. Mechanische und thermische Wirkungen beim Schleifen keramischer Werkstoffe. Dr.-Ing. Dissertation, Universität Hannover, 1998.